

Sheath and plasma parameters in a magnetized plasma system

BORNALI SINGHA, A SARMA and J CHUTIA

Institute of Advanced Study in Science and Technology, Khanapara, Guwahati 781 022, India

Email: iasst@gw1.vsnl.net.in

Abstract. The variation of electron temperature and plasma density in a magnetized N_2 plasma is studied experimentally in presence of a grid placed at the middle of the system. Plasma leaks through the negatively biased grid from the source region into the diffused region. It is observed that the electron temperature increases with the magnetic field in the diffused region whereas it decreases in the source region of the system for a constant grid biasing voltage. Also, investigation is done to see the change of electron temperature with grid biasing voltage for a constant magnetic field. This is accompanied by the study of the variation of sheath structure across the grid for different magnetic field and grid biasing voltage as well. It reveals that with increasing magnetic field and negative grid biasing voltage, the sheath thickness expands.

Keywords. Magnetic field; sheath; mesh grid; electron temperature.

PACS Nos 52.40.Hz

1. Introduction

The study of sheath formation between a magnetized plasma and a charged particle interaction wall has received considerable attention in the recent years. The main importance of this study is to see the change of the particle dynamics as well as the particle wall interaction in magnetized plasma. Irrespective of this, plasma sheath is making significant influence on the charged particles and the energy flux to the wall, which in turn greatly modifies the absorption, emission impurities and all other characteristics in the plasma.

A few number of theoretical papers are there, which mainly confine the study of magnetized sheath and pre-sheath. At the interface of plasma and any solid surface, there arises an electrostatic pre-sheath, a Debye sheath and a magnetic pre-sheath in a magnetized plasma. Chodura [1] has shown that when a magnetic field is present at some oblique angle to the solid surface, magnetic presheath is forming just before the Debye sheath, which produces a significant electric field in this region. He also showed that the development of this field make the plasma flow toward the surface of interacting wall. Stangeby [2] deduced a theoretical model for sheath formation viz. Bohm-Chodura plasma sheath criterion. He introduced a new condition to the flow velocity of ions entering the magnetic presheath, constrained to satisfy Chodura condition i.e. the ion velocity parallel to the magnetic field (B) must be equal or greater than the sonic velocity. He also confirmed the supersonic flow

velocity due to the magnetic presheath region in the $E \times B$ direction, which was earlier deduced by Chodura [1] and Riemann [3] by using quite different methods. In this contrast, Behnel [4] considered a magnetic field (B) which is parallel to the wall, provides the ion-charge exchange collision with the mean free path $\lambda \gg \rho_i$, where ρ_i is the ion-gyro radius. According to this model, there is no ion motion parallel to the magnetic field lines and no extra plasma pre-sheath was considered. However, the first general mechanism of magnetic pre-sheath was given by Riemann [3] on the basis of hydrodynamic fluid model, considering the case of oblique magnetic field and also collision effect. Mainly, he was able to show that the ion acceleration is generated by not only collision mechanism but also due to the combined effect of electric and magnetic field produced in a system. He found the dependence of potential distribution on the magnetic field and ion collision frequency in the pre-sheath region. The main effect of a strong magnetic field is to reduce the collisional presheath thickness as was approximated as ion Larmor radius but not the ion mean free path. In contrast to the case studied by Chodura [1], he also showed in his paper that an additional plasma pre-sheath is not required in the collisional case. Although, most of the studies of sheath and pre-sheath have investigated on collisional, unmagnetized plasmas, only a few have addressed on magnetic field effect, theoretically [5,6]. However, experimental study on sheath and pre-sheath in magnetized plasma is quite countable till date. Kim *et al* [7] have represented one experimental paper on sheath with magnetic and collisional effect. They have done their experiment in an inductively coupled source device with electron temperature many many times greater than the ion temperature and observed that the pre-sheath has a double structure composed of a collisional pre-sheath and a magnetic pre-sheath. This paper presents the change in plasma parameters (electron temperature and plasma density) in the source and diffused region of the plasma device with various magnetic field and grid biasing voltage. It also represents the characteristic behaviour of sheath in varying magnetic field and grid biasing voltage. The mode of this paper is as follows. Section 2 describes the experimental set up and diagnostic techniques. Experimental results and discussion are given in §3. Lastly, §4 yields the conclusive part of the paper.

2. Experimental set up

The experiment is performed in a hollow stainless steel cylinder of 1 meter in length and 0.2 meter in diameter. The schematic diagram of the experimental set up is shown in figure 1. A mesh grid of 95% transparency is introduced vertically at a distance of 46 cm apart from the right end of the chamber. It divides the system into two regions namely source region and diffused region. The chamber is evacuated by a rotary pump followed by a Diffstak pump to attain a base pressure of 1.5×10^{-6} Torr. N_2 gas is injected into the chamber at a working pressure of 0.75×10^{-4} Torr. Plasma is produced in the source region of the chamber by hot filament discharge phenomena. The plasma sustaining in the diffused region is controlled by its production in the source region, which are penetrating across the grid. In order to produce an external axial magnetic field, several turns of copper coils are wound in a region of 33 cm at the middle of the chamber. Due to the flow of the current in the coil ranging from 2.5 Ampere to 20 Ampere produces magnetic field of strengths from 66 gauss (G) to 515 gauss (G) accordingly in the system. An ion rich sheath is produced across the mesh grid by applying a negative voltage ($-V_g$) into it. The plasma density at the source region is of the order of $10^9/\text{cm}^3$, whereas it is somewhat lesser

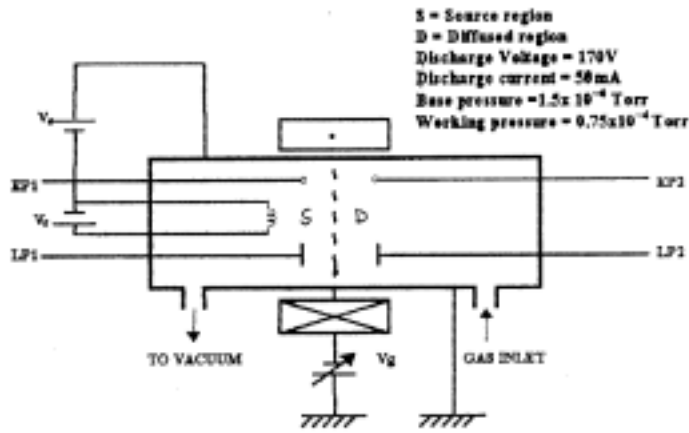


Figure 1. Schematic diagram of the experimental setup. *EP* = emissive probe, *LP* = Langmuir probe.

at the diffused region i.e. of the order of $10^8/\text{cm}^3$. Plane Langmuir probes (LP_1 and LP_2) and emissive probes (EP_1 and EP_2) are the two diagnostic tools used for the whole set of experiment. LP_1 and EP_1 are inserted in the source region at a distance of 6 cm away from the grid, whereas LP_2 and EP_2 are introduced in the diffused region at the same distance apart from the grid. With the help of the Langmuir probe, the plasma density and the temperature are measured. The emissive probes are used in this experiment to obtain the plasma potential profile on both sides of the grid. The floating potential technique [8] is mainly used to measure the potential profile by emissive probe.

3. Results and discussion

The dependence of the plasma parameters on the external magnetic field applied perpendicular to the grid and also upon the grid biasing voltage in the source and the diffused region is studied experimentally. The experiments are performed under the magnetic field ranging from 66 G to 515 G. For a particular magnetic field, a system can be said to be a weakly coupled or strongly coupled plasma if $\Gamma_e < 1$ or $\Gamma_e > 1$ where Γ_e is given by a relation

$$\Gamma_e = [e^2(4\pi n_e/3)^{1/3}]/kT_e. \quad (1)$$

Here, n_e and T_e are the plasma density and electron temperature respectively for a particular magnetic field strength (B). In this consideration, our plasma system is behaving as a weakly coupled one for the entire range of applied magnetic field. Experiments are performed for different grid biasing voltages ranging from -70 V onward to -100 V in presence of the above mentioned magnetic fields. Plasma is produced in the source region. The plasma density and electron temperature (T_{es}) in the source region are found to be of the order of 10^9 cm^{-3} and 2–6 eV respectively. The change of the electron temperature with magnetic field strength for $V_g = -80$ V in the source region is shown in figure 2.

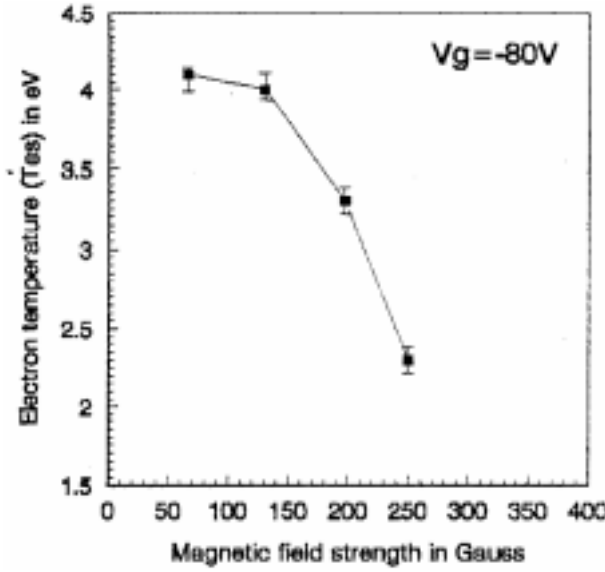


Figure 2. Variation of electron temperature with B at $V_g = -80$ V in the source region.

It is found that though electron temperature decreases with B , the quantitative values are lesser in comparison to that of the diffused region (table 1).

Due to the introduction of the magnetic field, the particle dynamics totally changes. In its presence, particles are constrained to gyrate about the lines of force so that they move at different rates along and across the field. Hence, this introduces an anisotropy, which makes the particle flow at least two-dimensional. In this magnetized plasma experiment, a plane Langmuir probe is used as detector [9]. With the increase of magnetic field, the electron temperature in the source region reduces (figure 2). As the external magnetic field increases, plasma particles are confined more and more as a consequence of their changing diffusion pattern. In presence of the magnetic field, particles diffuse along the magnetic field simply due to their mobility, but in the transverse direction, they diffuse at the step-length of the Larmor gyro radius. Hence, as soon as magnetic field increases, Larmor gyro radius is lowered and finally less number of particles can escape from the source region toward the boundary wall. The diffusion of the particles across and along the magnetic field can be understood [10] from the following equations.

$$D = KT\nu/mw_c^2 \approx V_{th}^2 r_L^2 \nu / V_{th}^2 \approx r_L^2 / \tau \quad (2)$$

$$D_{\parallel} = KT/m\nu \approx V_{th}^2 \tau \approx \lambda_m^2 / \tau. \quad (3)$$

Here, D and D_{\parallel} denotes the diffusion coefficients across and along the magnetic field direction respectively. In the above two equations, K is the Boltzmann constant, T is the temperature of the plasma particles, ν is the collision frequency, m is the particle mass, w_c is the cyclotron frequency, V_{th} is the thermal velocity of the particles, r_L is the Larmor radius, λ_m is the mean free path and τ is the time between two collisions.

Table 1. Electron temperature at $V_g = -80$ V with various B in source region.

Magnetic field strength in G	66	130	197	250
Electron temperature in eV	4.1	4	3.3	2.3

Table 2. Electron temperature at $B = 130$ G with various $-V_g$ in source region.

Grid bias voltage in V	-70	-80	-90	-100
Electron temperature in eV	3.55	4	5	7

Table 3. Electron temperature at $V_g = -80$ V with various B in diffused region.

Magnetic field strength in G	66	130	197	250
Electron temperature in eV	8.5	9.45	11.55	12.8

Table 4. Electron temperature at $B = 130$ G with various $-V_g$ in diffused region.

Grid bias voltage in V	-70	-80	-90	-100
Electron temperature in eV	10.9	9.45	10.5	7.15

Table 5. Plasma density at $V_g = -80$ V with various B in source region.

Magnetic field strength in G	66	130	197	250
Plasma density in cm^{-3}	0.16×10^9	0.19×10^9	0.22×10^9	0.24×10^9

Table 6. Plasma density at $B = 66$ G with various $-V_g$ in source region.

Grid bias voltage in V	-70	-80	-90	-100
Plasma density in cm^{-3}	0.22×10^9	0.16×10^9	0.16×10^9	0.15×10^9

Table 7. Plasma density at $V_g = -80$ V with various B in diffused region.

Magnetic field strength in G	66	130	197	250
Plasma density in cm^{-3}	0.3×10^8	0.2×10^8	0.12×10^8	0.16×10^8

Table 8. Plasma density at $B = 130$ G with various $-V_g$ in diffused region.

Grid bias voltage in V	-70	-80	-90	-100
Plasma density in cm^{-3}	0.3×10^8	0.2×10^8	0.136×10^8	0.086×10^8

Table 9. Electron-neutral collision frequency at $V_g = -80$ V with various B in the source region.

Magnetic field strength in G	66	130	197	250
Electron-neutral collision frequency in sec^{-1}	485	600	928	1438

Table 10. Electron-neutral collision frequency at $B = 130$ G with various $-V_g$ in the source region.

Grid bias voltage in V	-70	-80	-90	-100
Electron-neutral collision frequency in sec^{-1}	751	600	523	219

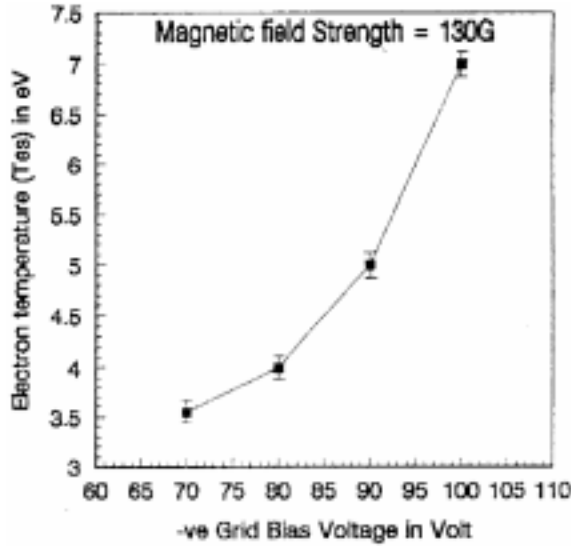


Figure 3. Variation of electron temperature with $-V_g$ at $B = 130$ G in the source region.

Due to the enhancement of the plasma density (table 5) electron neutral collision dominates which in turn, causes more energy dissipation and hence lowers the electron temperature (table 9).

The change of electron temperature with V_g at a constant magnetic field strength is presented in figure 3. However, it shows that Tes gradually increases with V_g at a particular magnetic field (table 2). Under this condition, electron-neutral collision reduces which is found out quantitatively and shown in table 10. Also variation of plasma density under this condition is given in table 6. Figures 4 and 5 give the structures of the potential profiles measured by the emissive probes near the grid in the diffused region and thereby describing the sheath thickness at varying V_g and B respectively.

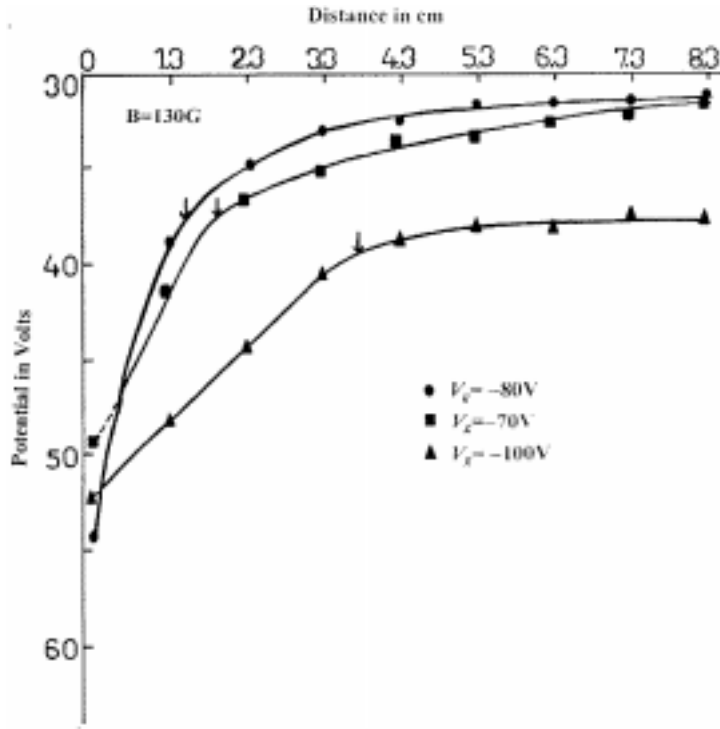


Figure 4. Potential profile near the grid at the diffused region with $B = 130$ G and varying $-V_g$.

It is clearly seen from the figures that sheath thickness increases with V_g and B [\downarrow (arrow mark) in the potential profile indicates the sheath edge]. It is well established that increasing V_g negatively enhances the ion rich sheath width across the grid considerably [11]. The ions forming the sheath across the grid, are moving with a velocity equal to or greater than the ion acoustic velocity (C_s), in order to satisfy the minimum Bohm sheath criterion. For a fixed V_g , when more and more magnetic field is applied, gyro radius of both ions and electrons are reduced gradually. But at the same time gyro frequencies of both the species increase. Furthermore, the external magnetic field applied to the plasma chamber is not homogeneous in both the axial and radial direction of the chamber. The mapping of the magnetic field in both the directions are shown in figures 6 and 7. Due to these magnetic field gradients, a grad B drift of the particles [10] occurs as followed by the equation,

$$V_{\nabla B} = \pm 1/2 v r_L (B \times \nabla B) / B^2. \quad (4)$$

The direction of the drift velocity of both the species will be decided by the charge of the species. However, since the grid is maintained at a negative biased voltage, preferably the ions are drifting toward it and due to their greater inertia, they simply cross over to the diffused region. But they are gradually accumulated there as the applied negative voltage attracts them again. As soon as B increases, gyro Larmor radius of ions gradually

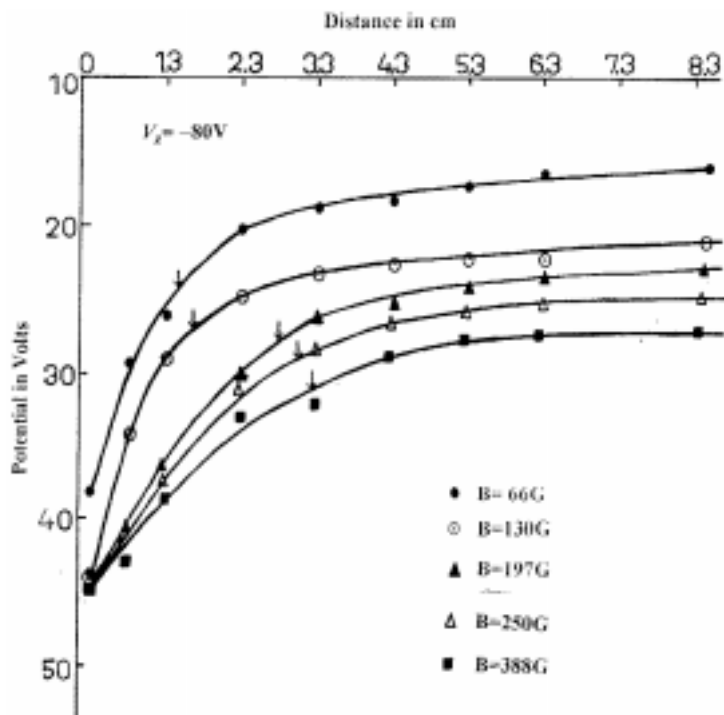


Figure 5. Potential profile near the grid at the diffused region with $V_g = -80$ V and varying B .

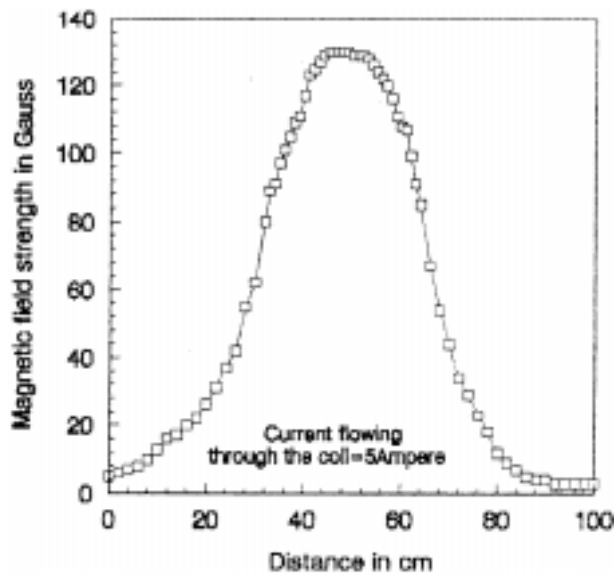


Figure 6. Axial profile of the external magnetic field throughout the chamber length when current flowing through the coil is 5 Ampere.

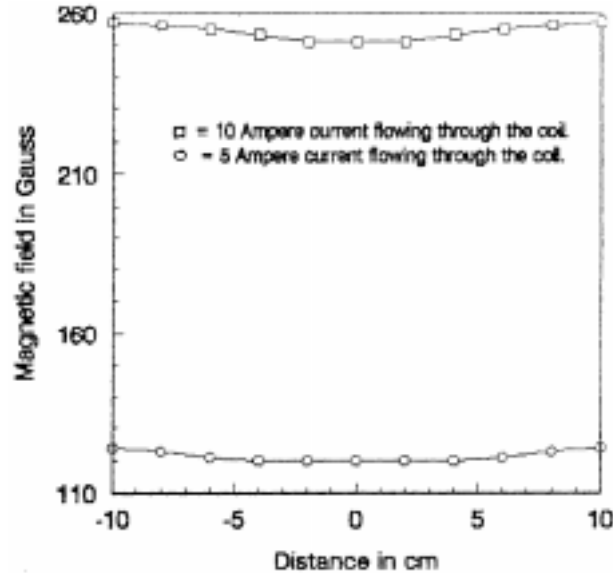


Figure 7. Radial profile of the external magnetic field at the position of 55 cm from the right end of the chamber when current flowing through the coil are 5 Ampere and 10 Ampere respectively. (0 on the X-axis denotes the centre of the cylindrical cross section).

attenuate which allows more ion particles to drift through the mesh size of the grid. Also, it is seen from the eq. (4) that as B increases, the ratio $\nabla B/B$ increases. Taking into account all these effects, it can be concluded that the sheath thickness at the diffused region enhances under both the conditions of external magnetic field and grid biasing voltage.

Plasma produced in the source region penetrates through the negatively biased grid and is distributed in the diffused region under the influences of magnetic field and v_g as well. The variation of the plasma parameters i.e. the electron temperature and the plasma density at different condition is observed experimentally in this region (tables 3, 4, 7 and 8). Figure 8 provides the dependence of the electron temperature (T_{ed}) on B when grid is biased at -80 V. It is found that T_{ed} increases due to the increase of B . Also, the value of electron temperature in this region is found to be much higher than that in the source region. The reason for this can be explained as follows. Since the grid is constantly given a negative voltage, an ion rich sheath is formed near it as stated earlier which provides a potential barrier for the electrons to drift from source region to diffused region. So, only those high energetic electrons can drift to the diffused region which can overcome this potential barrier. Moreover, as the ionization potential of N_2 is higher, the electrons are not able to take part in the secondary ionization of the neutral atom keeping their energy intake. The enhancement of electron temperature in the diffused region with B is mainly attributed due to the reduction of electron gyro Larmor radius. It is already mentioned that the plasma density in this region is lesser as there is no source of plasma production. Hence, in the environment of rarely

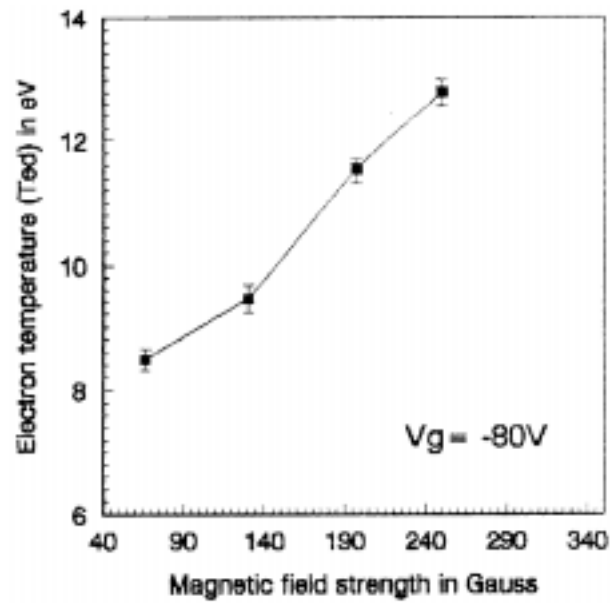


Figure 8. Variation of electron temperature with B at $V_g = -80$ V in the diffused region.

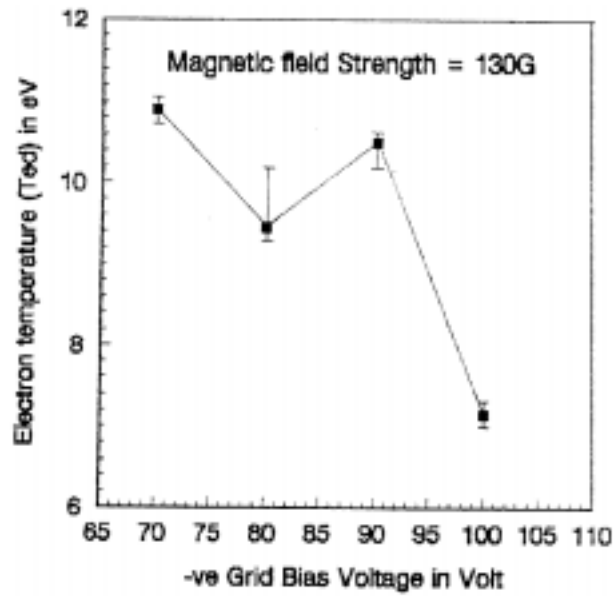


Figure 9. Variation of electron temperature with $-V_g$ at $B = 130$ G in the diffused region.

Table 11. Electron-neutral collision frequency at $V_g = -80$ V with various B in the diffused region.

Magnetic field strength in G	66	130	197	250
Electron-neutral collision frequency in sec^{-1}	30	20	8	6

Table 12. Electron-neutral collision frequency at $B = 130$ G with various $-V_g$ in the diffused region.

Grid bias voltage in V	-70	-80	-90	-100
Electron-neutral collision frequency in sec^{-1}	19	20	21	24

populated plasma, as electron Larmor radius also decreases with B , so, the probability of electron neutral collision reduces more (table 11). As a consequence of which, electron temperature rises up.

While, the phenomenon has completely changed with varying V_g i.e. decreases with more negative V_g . These results are plotted in figure 9. The change of T_{ed} with V_g can be explained as follows. The existence of the plasma in the diffused region is mainly controlled by the plasma produced in the source region. It is mentioned that T_{ed} increases with B . However, T_{ed} is reduced while more $-V_g$ is applied. In this case, as sheath thickness increases corresponding to more $-V_g$, ion flow as well as electron flow due to ambipolar drift toward the grid is becoming more. Due to this reason, probability of electron-neutral collision in that region is also more (table 12). As a consequence of which electrons dissipate energy thereby lowering T_{ed} slightly. The variation of T_{ed} with $-V_g$ is comparatively smaller than that with B since the grid bias mainly affects potential energy of the electrons rather than the kinetic energy.

4. Conclusion

The effect of external magnetic field and the grid biasing voltage for the considerable change of the plasma parameters in a magnetized plasma system has been studied. In the weakly coupled plasma system, the kinetic energy of the electron is playing a key role for the variation of electron temperature with B in the source and diffused region. The experiment concludes that T_{es} decreases with B while T_{ed} changes oppositely, for fixed $-V_g$. On the other hand, the sheath thickness increases with more negative grid biasing voltage which in turn varies the electron temperature in both the regions in an opposite manner. Under this condition, T_{es} increases with the increase of $-V_g$ for a constant B and vice versa is happening in the diffused region. Simultaneously, the study also reveals that any changes in the plasma parameters are more effective in the diffused region than in the source region due to both B and $-V_g$.

Acknowledgement

Authors are thankful to the Department of Science and Technology, Government of India for the financial support.

References

- [1] R Chodura, *Phys. Fluids* **25**, 1628 (1982)
- [2] P C Stangeby, *Phys. Plasmas* **2(3)**, 702 (1995)
- [3] K-U Riemann, *Phys. Plasmas* **1**, 552 (1994)
- [4] J Behnel, Ph. D. Thesis (Ruhr University, Bochum, 1985)
- [5] K-U Riemann, *J. Phys.* **D24**, 493 (1991)
- [6] G L Main, *Phys. Fluids* **30**, 1800 (1987)
- [7] G H Kim, N Hershkowitz, D A Diebotd and M H Cho, *Phys. Plasmas* **2(8)**, 3222 (1995)
- [8] J R Smith, N Hershkowitz and P Coakley, *Rev. Sci. Instrum.* **50(2)**, 210 (1979)
- [9] I H Hutchinson, *Principles of Plasma Diagnostics* (Cambridge University Press, Cambridge, 1990)
- [10] F F Chen, *Introduction to Plasma Physics and Controlled Fusion* (Plenum Press, New York, 1984) vol. 1
- [11] A Sarma, H Bailung and J Chutia, *Phys. Plasmas* **3(8)**, 3245 (1996)